Supporting information for

Rapid, multiplexed phosphoprotein profiling using silicon photonic sensor arrays

James H. Wade[1], Aurora T. Alsop[1], Nicholas R. Vertin[1], Hongwei Yang[2], Mark D. Johnson[2], and Ryan C. Bailey[1]*

[1]Department of Chemistry, University of Illinois at Urbana-Champaign, 600 S. Mathews Ave., Urbana, IL, 61801

[2]Department of Neurological Surgery, Brigham and Women's Hospital and Harvard Medical School, Boston, MA 02115

Table S1. List of protein targets ……. S2

Table S2. Antibodies for protein targets ……... S3

Table S3. Logistic fit parameters for β-catenin protein standard curve …….. S4

Table S4. Standard scores (z-score) corresponding to the heat map form Fig. 4a …… S5

Table S5. Standard scores (z-score) corresponding to the heat map form Fig. 5a …… S6

Table S6. Standard scores (z-score) corresponding to the heat map form Fig. 5b …… S7

Figure S1. Sensor array capture spotting map ……..…….…. S8

Figure S2. Enzymatically-enhanced assay scheme ……..……... S9

Figure S3. Visualization of real-time binding events for β-catenin detection ……..... S10

Figure S4. Technical and biological variance of platform …… S11

Figure S5. Phosphoprotein-based clustering of primary glioma tumor specimens ….. S12

Figure S6. Validation of antibody pairs with western blotting ……. S13

Figure S7. Fluidic interface and cartridge assembly ……..…. S14

Table S1: **List of protein targets**

Target	**Pathway**
β-Catenin	Wnt/ β-Catenin
phospho-Rb Ser780	cell cycle
phospho-Rb Ser807/811	cell cycle
phospho-Akt Ser473	PI3K/AKT
phospho-Akt Thr308	PI3K/AKT
S6 ribosomal protein	PI3K/AKT & translation
phospho-S6 Ser235/236	PI3K/AKT & translation
phsopho-S6 Ser240/244	PI3K/AKT & translation
TSC1/2	PI3K/AKT
phospho-TSC2 Thr1462	PI3K/AKT
phospho-mTOR Ser2448	PI3K/AKT
phospho-p44/42 MAPK (Erk1/2) Thr202/Tyr204	RAS/RAF/MAPK

Table S2: Antibodies for protein targets

Target	Clone	Role	Catalog Number
β-Catenin	D10A8	Capture	8480
β-Catenin	L87A12	Tracer	2698
Tuberin/TSC2	D93F12	Tracer	4308
Tuberin/TSC2	28A7	Capture/Tracer	3635
Phospho-TSC2 Thr1462	5B12	Capture	3617
S6 Ribosomal Protein	5G10	Capture/Tracer	2217
S6 Ribosomal Protein	21A12	Tracer	2355
Phospho-S6 Ser235/236	D57.2.2E	Capture	4858
Phospho-S6 Ser240/244	D68F8	Capture	5364
mTOR	7C10	Tracer	2983
Phospho-mTOR Ser2448	D9C2	Capture	5536
Akt (pan)	C67E7	Tracer	4691
Akt (pan)	11E7	Tracer	4685
Phospho-Akt Ser473	D93	Capture	4060
Phospho-Akt Thr308	L32A4	Capture	5106
p44/42 MAPK (Erk1/2)	137F5	Tracer	4695
Phospho-p44/42 MAPK (Erk1/2) Thr202/Tyr204	D13.14.4E	Capture	4370
Rb	4H1	Tracer	9309
Phospho-Rb Ser780	D59B7	Capture	8180
Phospho-Rb Ser807/811	D20B12	Capture	8516

Table S3: Logistic fit parameters for β-catenin protein standard curve

Model	Logistic	
Equation	$y = A_2 + \frac{A_1 - A_2}{1 + \left(\frac{x}{x_0}\right)^p}$	
Reduced χ^2	0.03698	
Adj. r^2	0.9986	
	Value	**Standard Error**
A_1 (Δpm)	1.91847	0.55574
A_2 (Δpm)	15184.89437	348.45725
x_0 (pM)	71.76693	8.31686
p	1.13617	0.02733

Table S4: Standard scores (z-score) corresponding to the heat map form Fig. 4a

	U87	LN228	T98	U343	U251
BETA-CATENIN	0.14	-0.13	1.35	0.09	-1.46
P-AKT S473	-0.50	-0.66	1.60	-0.79	0.35
P-AKT T308	-0.27	-1.02	1.60	-0.53	0.23
P-MTOR S2448	-0.97	-1.19	0.94	0.73	0.49
P-P44/42 MAPK	-0.35	-0.14	1.63	-1.10	-0.03
P-RB S780	-0.09	-0.14	1.68	-0.49	-0.96
P-RB S807/811	-1.43	-0.16	0.25	-0.03	1.37
P-S6 S235/236	-1.49	0.34	1.10	-0.45	0.50
P-S6 S240/244	-1.22	0.09	1.22	-0.76	0.67
P-TSC2 T1462	0.23	-0.79	1.32	-1.18	0.42
S6	0.20	-0.13	1.55	-0.46	-1.15
TSC2	0.48	-0.99	-0.34	-0.65	1.50

Table S5: Standard scores (z-score) corresponding to the heat map form Fig. 5a

	(-)-SERUM LN229	(+)-SERUM LN229	VEGF LN229	EGF LN229	RAPAMYCIN LN229	WORTMANNIN LN229	(-)-SERUM U87	(+)-SERUM U87	VEGF U87	EGF U87	RAPAMYCIN U87	WORTMANNIN U87
BETA-CATENIN	1.27	-0.45	0.39	0.86	0.82	1.66	-1.44	-0.63	-0.13	-1.30	-0.28	-0.77
P-AKT S473	-0.54	0.92	-0.97	1.13	-1.54	-1.34	0.47	1.36	0.14	-0.21	1.05	-0.47
P-AKT T308	-0.57	-1.64	-0.10	1.87	-0.49	0.30	-0.18	1.08	-0.38	-0.56	1.39	-0.73
P-MTOR S2448	0.53	-1.30	0.13	1.75	-1.48	-1.10	-0.01	0.09	0.90	-0.81	0.98	0.34
P-P44/42 MAPK	0.35	-1.81	0.09	1.08	-0.81	0.45	-0.92	1.83	-0.61	-0.71	0.55	0.49
P-RB S780	0.53	1.11	0.63	1.51	0.96	0.75	-0.86	-0.69	-1.08	-0.67	-1.30	-0.89
P-RB S807/811	0.82	1.11	0.59	1.21	0.75	1.07	-0.87	-0.90	-1.10	-0.47	-1.35	-0.87
P-S6 S235/236	-0.69	0.42	-0.51	0.18	-1.58	-0.56	1.30	1.12	1.08	0.01	-1.58	0.80
P-S6 S240/244	-0.16	0.13	-0.77	0.45	-1.96	0.15	1.05	1.41	1.13	-0.34	-1.33	0.24
P-TSC2 T1462	0.71	1.77	0.38	0.51	-0.09	1.27	0.28	-0.97	-0.65	-1.47	-1.19	-0.55
S6 (5G10)	-0.11	0.15	-0.32	2.61	-0.28	0.49	-1.23	-0.54	-1.07	-0.62	0.40	0.51
TSC2	1.18	-0.95	0.75	1.35	0.50	1.32	0.05	-0.76	-0.77	-1.59	-0.40	-0.68

Table S6: Standard scores (z-score) corresponding to the heat map form Fig. 5b

	30304	21985	21225	86941	98131	43096
BETA-CATENIN	0.47	-0.86	1.34	0.76	-0.53	-1.18
P-AKT S473	-1.29	0.61	0.19	1.52	-0.29	-0.74
P-AKT T308	0.34	0.99	-1.15	0.78	0.39	-1.35
P-MTOR S2448	-1.04	0.31	0.16	1.61	0.05	-1.09
P-P44/42 MAPK	-0.81	-0.15	-0.32	1.93	-0.70	0.05
P-RB S780	-1.03	1.10	-0.05	1.25	-0.23	-1.05
P-RB S807/811	0.06	1.93	-0.84	-0.59	-0.11	-0.45
P-S6 S235/236	0.27	1.18	-1.11	1.06	-0.40	-1.01
P-S6 S240/244	-0.93	0.25	0.16	1.77	-0.34	-0.90
P-TSC2 T1462	0.47	1.09	-1.60	0.04	0.72	-0.71
S6	1.18	-0.73	0.61	0.90	-0.99	-0.96
TSC2	1.63	-0.70	-0.58	-0.53	0.87	-0.68

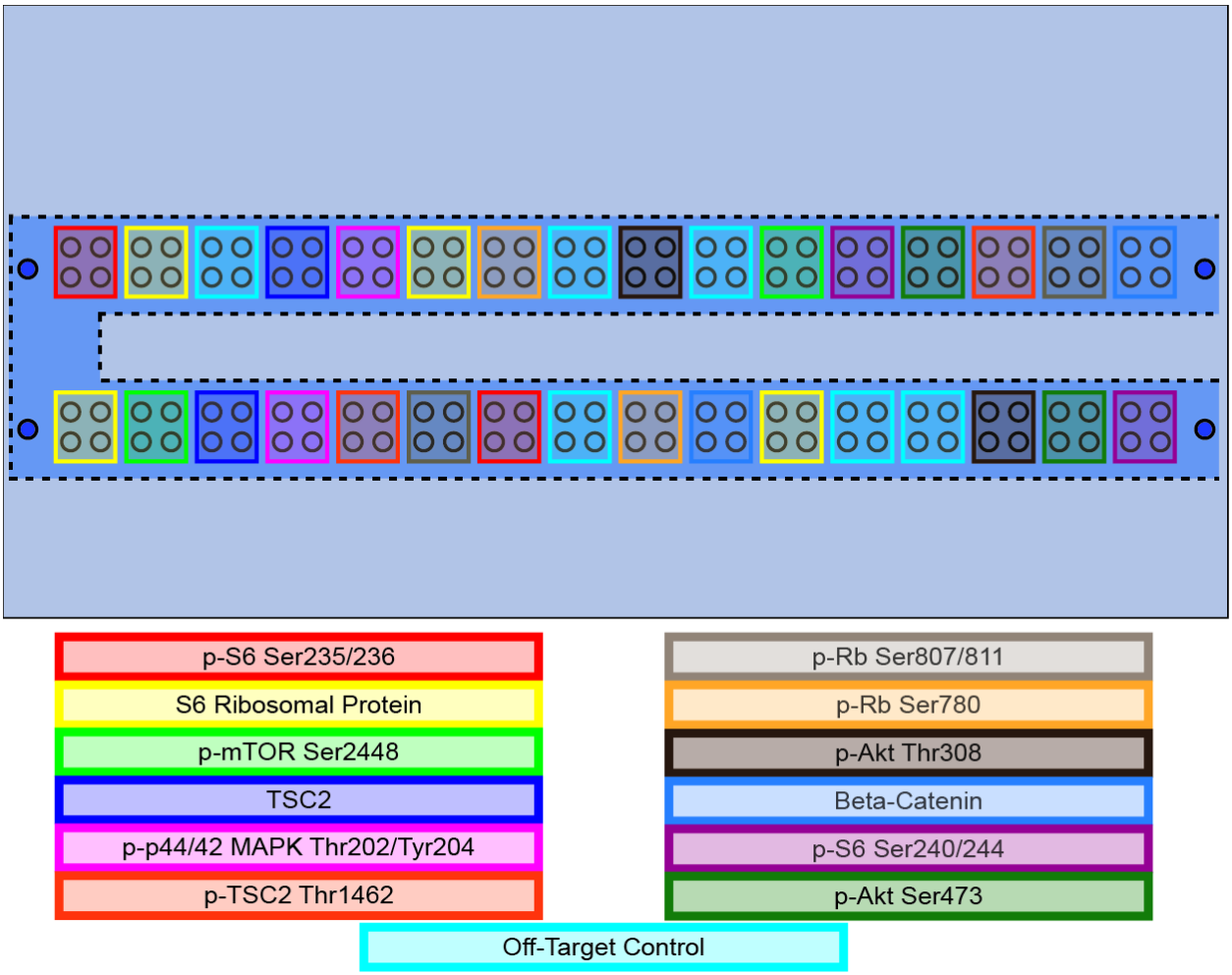

Figure S1

Sensor array capture spotting map. The 4 x 6 mm silicon photonic chip contains 132 active rings and 4 thermal controls. Active rings are arranged in clusters of 4, and the chips contains 32 clusters of rings. Unlike active rings, thermal control rings are covered with a fluoropolymer cladding layer. The chip schematic shows the layout for antibody spotting using a robotic microspotter. The fluidic path across the chip is also highlighted by the dashed lines.

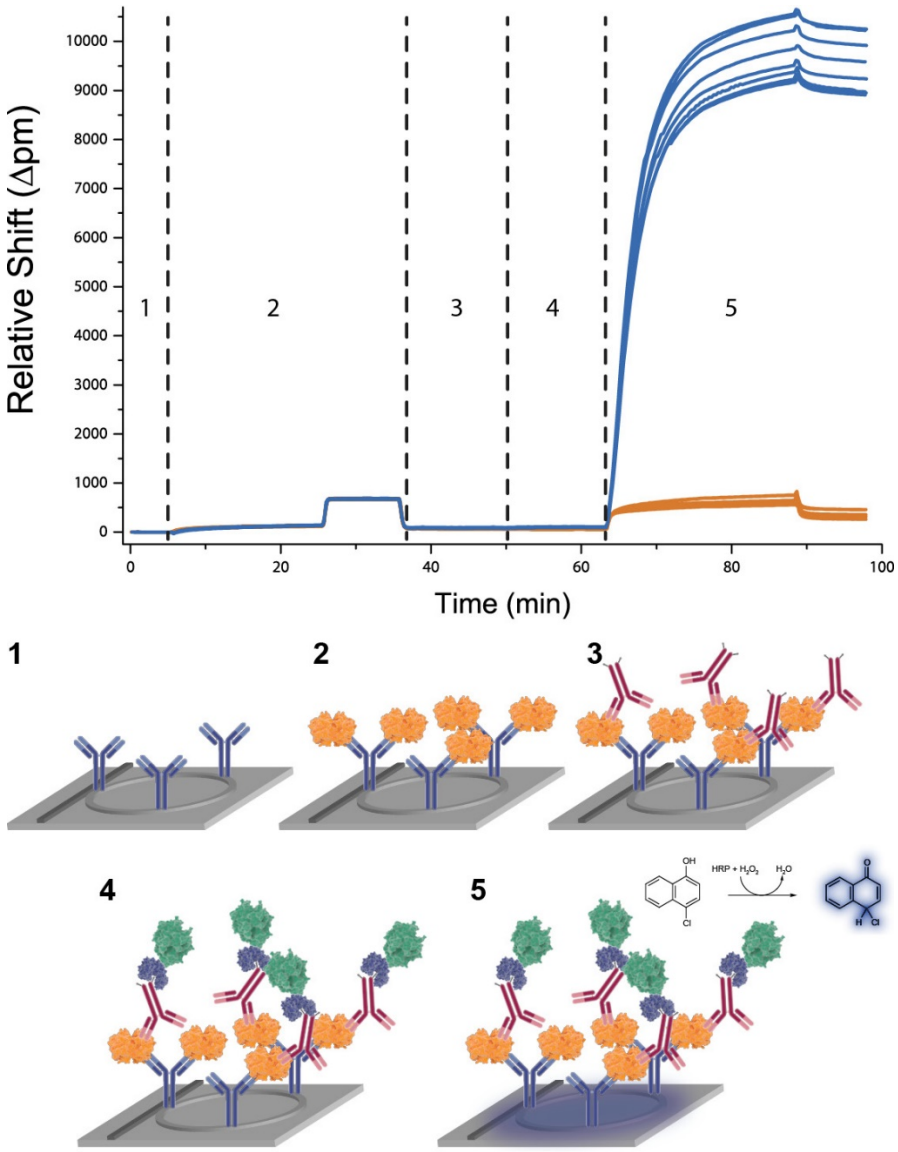

Figure S2

Enzymatically-enhanced assay scheme. Multiplexed protein detection in cell lysate is a 2 h assay consisting of 3 binding steps and enzymatic signal enhancement. The assay consists of (**1**) chip functionalization and protein blocking steps, (**2**) analyte capture from cell lysate, (**3**) binding of biotinylated tracer antibody, (**4**) binding of SA-HRP conjugate to biotinylated tracer, and (**5**) enzymatic signal enhancement via oxidation of 4CN to the insoluble product, 4-chloronaphton. The top panel shows results from on-target (blue) and off-target (orange) for detection of β-catenin in 10 mM PBST/B buffer (Online Methods). Each trace represents an individual sensor.

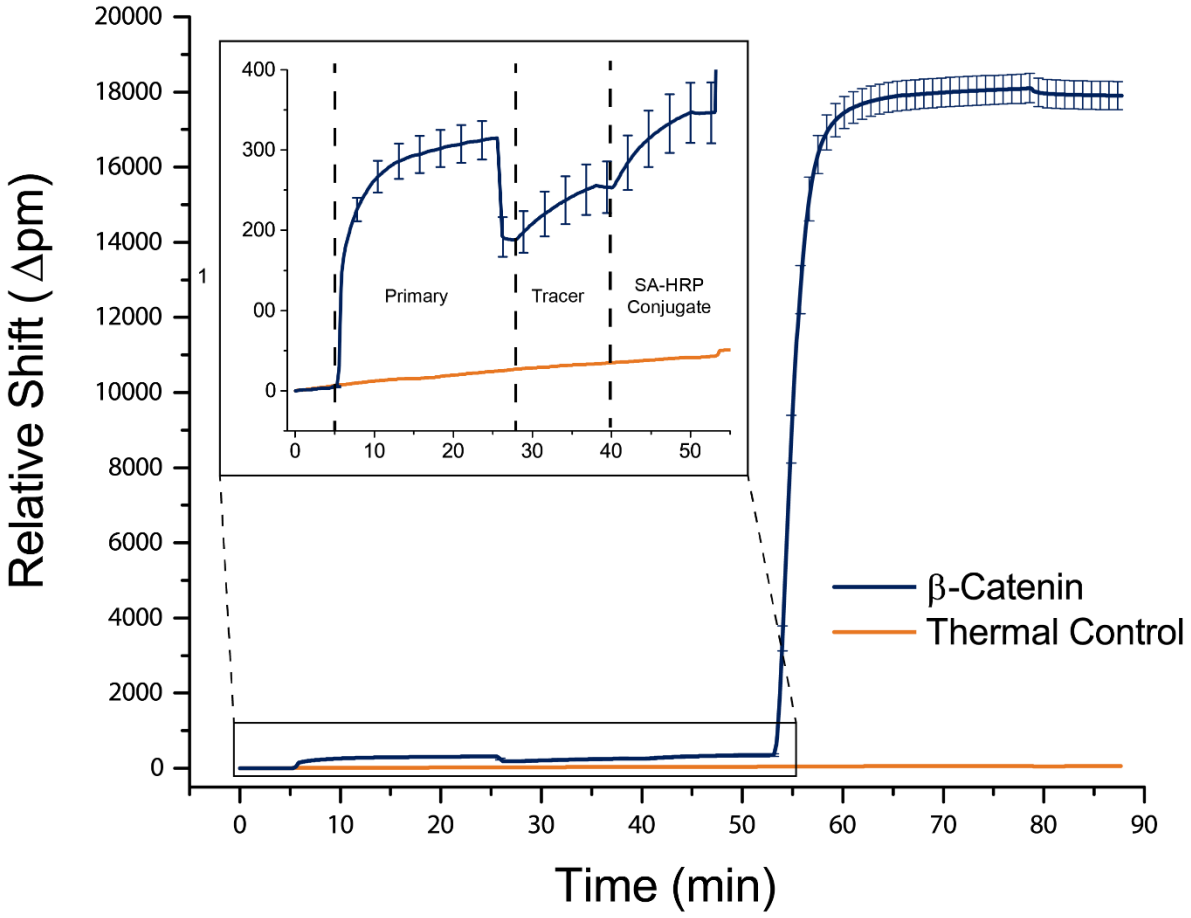

Figure S3

Visualization of real-time binding events of β-catenin. The response from β-Catenin, shown in blue, can be seen for each of the binding events during the assay. The inset shows analyte binding (in buffer) to capture antibodies, biotinylated tracer antibodies binding to captured analyte, and streptavidin-horseradish peroxidase (SA-HRP) binding to the biotinylated tracer. The final step visible in the larger plot shows the oxidation of 4CN, resulting in the large increase in signal between 50 and 60 min. Error bars represent ± s.d. (n=8 technical replicates). The orange trace shows data from the on-chip thermal control sensor.

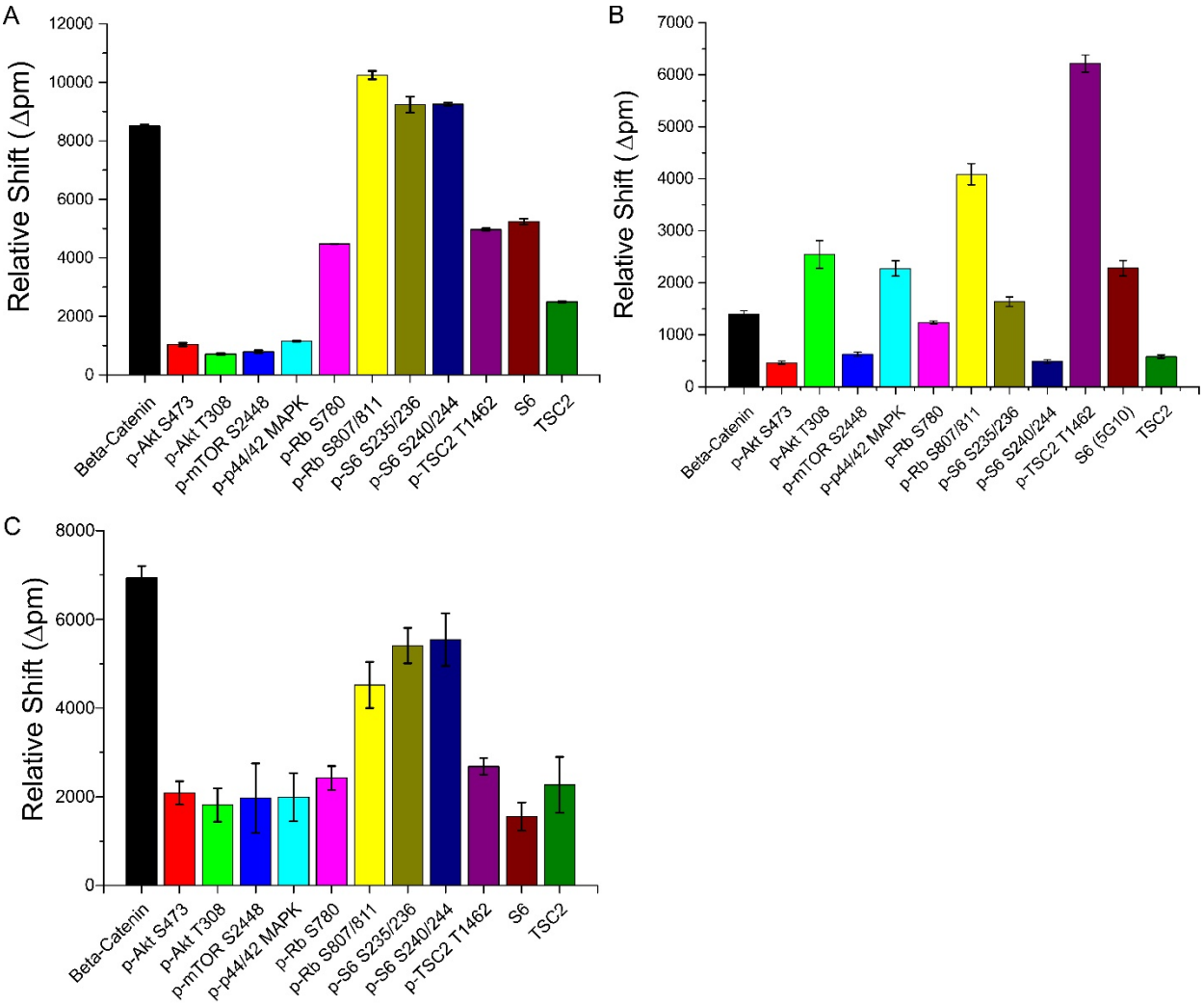

Figure S4

Technical and biological variance of platform for detecting in tissue culture and tumor homogenate samples. (**A**) Analysis of identical samples from LN-229 cell lysate shows an average technical variance of 2.3% (N = 3). (**B**) Triplicate measurements of a single patient sample show average technical variance of 5.9%. (**C**) Cell lysate analysis from the U87 cell line collected at different passage numbers shows an average biological variance of 17.9%. For all panels, error bars represent ± s.d. (n=3 different sensor substrates).

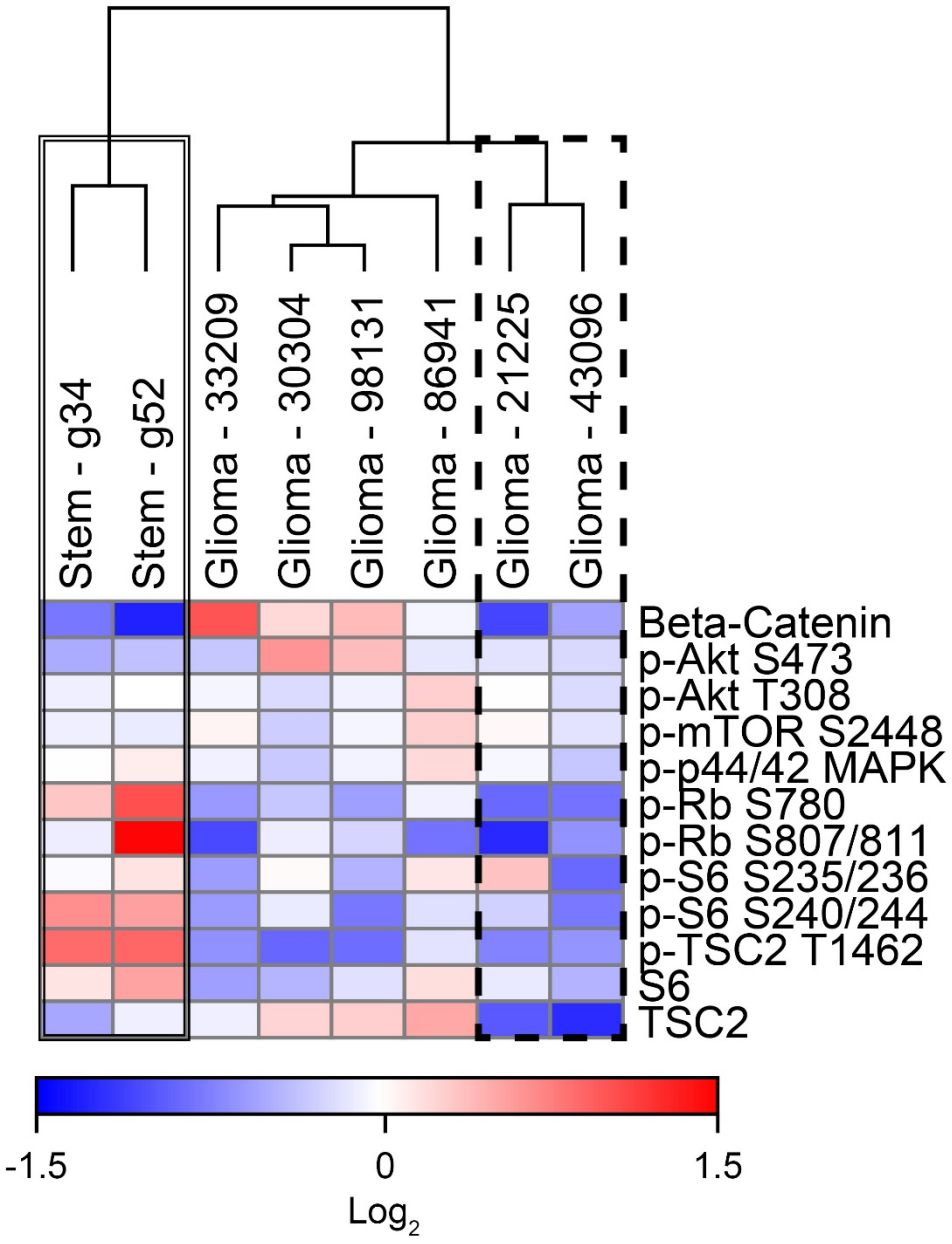

Figure S5

Phosphoprotein-based clustering of primary glioma tumor specimens. Unsupervised hierarchical clustering was performed for the 6 resected glioma tumor specimens and 2 primary glioma stem cells lines. The clustering reveals two key findings: (1) primary stem cell lines have demonstrate key differences between resected tumor specimens (double-lined outline) and (2) patient samples 21225 and 43096 were clustered as separate from the rest of the patient samples (dashed outline). We do not which to imply conclusive sorting capabilities based on such a small patient cohort, but the results provide promising result for the application of the technology to a clinical setting. Analysis time for each sample is <2 h, and the method was highly reproducible with an average coefficient of variance for the 12 targets was 5.9%.

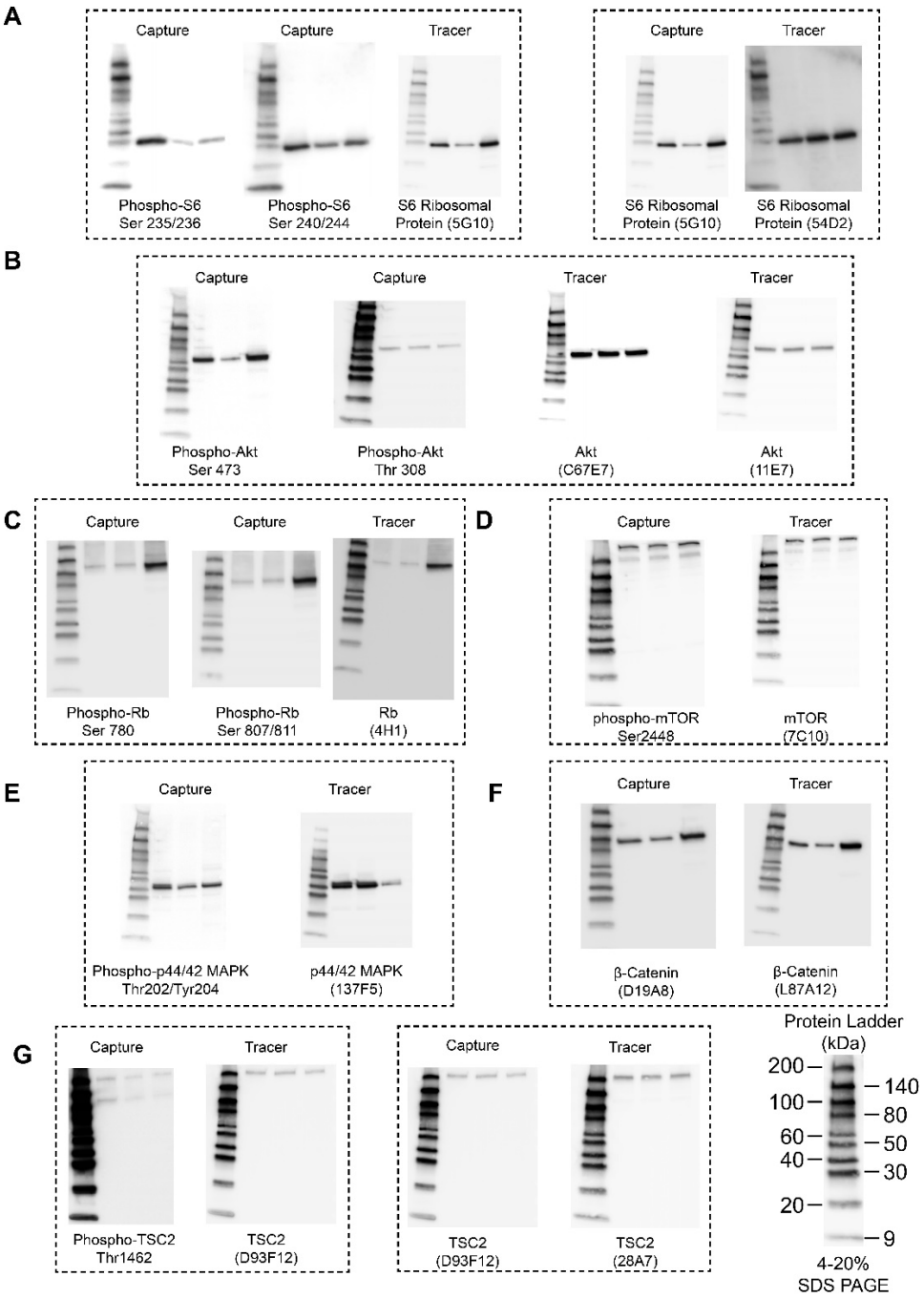

Figure S6

Validation of antibody pairs with western blotting. All antibodies were validated against cell lysate from 3 different glioma cell line models. For all images, the layout from left to right is as follows: biotinylated protein ladder, U87, LN-229, and U-251.The hyphenated boxes represent antibody pair used for analyte detection on the microring resonator platform. Antibody sandwich pairs were validated for (**A**) S6 ribosomal protein, (**B**) Akt, (**C**) retinoblastoma protein (Rb), (**D**) mTOR, (**E**) p44/42 MAPK (**F**) β-catenin, and (**G**) tuberous sclerosis 2 (TSC2).

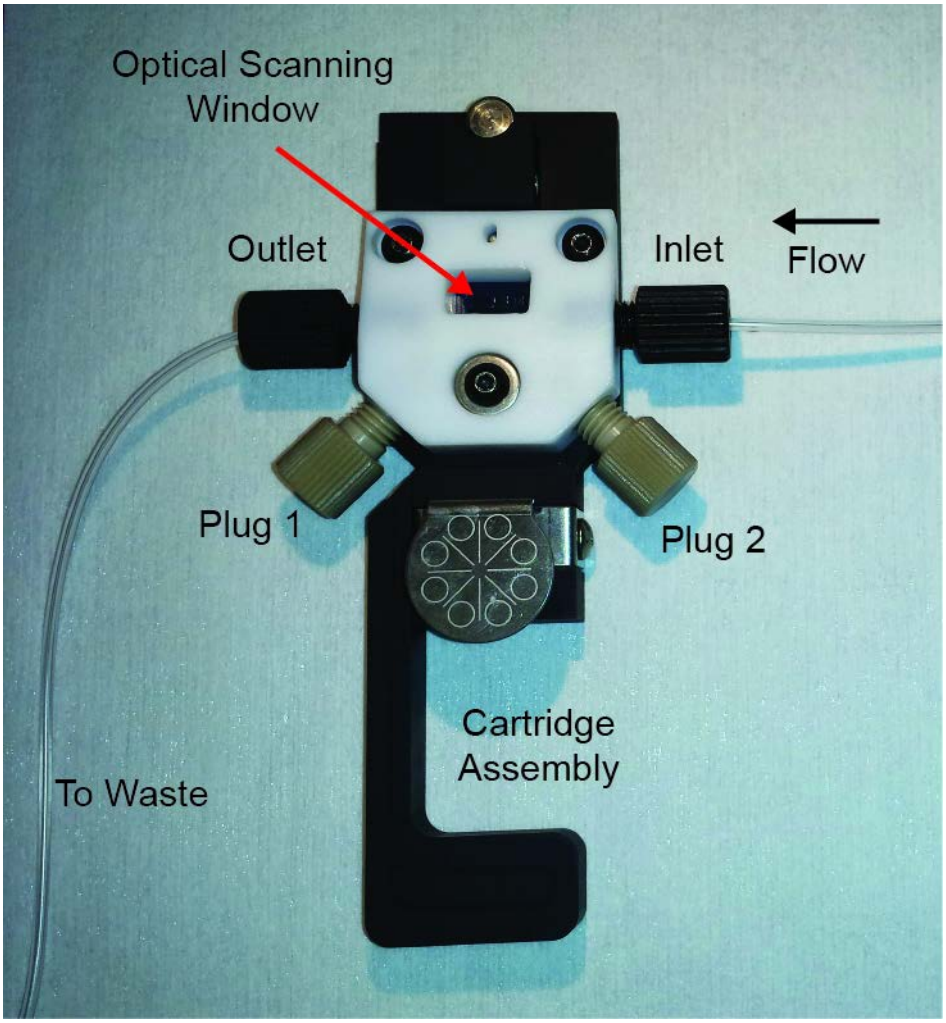

Figure S7

*Fluidic interface and cartridge assembly***.** Fluidic control is achieved by sandwiching the chip between a chip holder and fluidic gasket that is laser cut into a U-shaped channel. In order from bottom to top, the cartridge assembly consists of an aluminum cartridge holder, SOI sensor chip, Mylar fluidic gasket, and Teflon cartridge top. The cartridge assembly allows for multiple flow configuration, and 2 PEEK plugs are used to block the unused fluidic port. The optical scanning window allows for the sequential interrogation of each microring using a tunable diode laser.